

Modeling of cascaded high isolation bidirectional amplification in long-distance fiber-optic time and frequency synchronization system

Kuan-Lin Mu(穆宽林), Xing Chen(陈星), Zheng-Kang Wang(王正康), Yao-Jun Qiao(乔耀军), and Song Yu(喻松)
Citation: Chin. Phys. B, 2021, 30 (**7**): 074208. DOI: 10.1088/1674-1056/abf105
Journal homepage: http://cpb.iphy.ac.cn; http://iopscience.iop.org/cpb

What follows is a list of articles you may be interested in

Real time high accuracy phase contrast imaging with parallel acquisition speckle tracking

Zhe Hu(胡哲), Wen-Qiang Hua(滑文强), and Jie Wang(王 劼)
Chin. Phys. B, 2021, 30 (**6**): 064201. DOI: 10.1088/1674-1056/abee08

Microwave frequency transfer over a 112-km urban fiber link based on electronic phase compensation

Wen-Xiang Xue(薛文祥), Wen-Yu Zhao(赵文宇), Hong-Lei Quan(全洪雷), Cui-Chen Zhao(赵粹臣), Yan Xing(邢燕), Hai-Feng Jiang(姜海峰), Shou-Gang Zhang(张首刚)
Chin. Phys. B, 2020, 29 (**6**): 064209. DOI: 10.1088/1674-1056/ab84d6

Cascaded optical frequency transfer over 500-km fiber link using regenerative amplifier

Xue Deng(邓雪), Dong-Dong Jiao(焦东东), Jie Liu(刘杰), Qi Zang(臧琦), Xiang Zhang(张翔), Dan Wang(王丹), Jing Gao(高静), Rui-Fang Dong(董瑞芳), Tao Liu(刘涛), Shou-Gang Zhang(张首刚)
Chin. Phys. B, 2020, 29 (**5**): 054205. DOI: 10.1088/1674-1056/ab7b4f

Acquisition performance analysis for intersatellite optical communications with vibration influence

Jing Ma(马晶), Gaoyuan Lu(陆高原), Siyuan Yu(于思源), Liying Tan(谭立英), Yulong Fu(付玉龙), Fajun Li(黎发军)
Chin. Phys. B, 2020, 29 (**1**): 014205. DOI: 10.1088/1674-1056/ab577e

Wavelength tunable ultra-short pulses based on a flat broadbandspectrum generated in a nonlinear ytterbium-dopedfiber amplifier

Run-Qin Xu(徐润亲), Zi-Kai Dong(董自凯), Jin-Rong Tian(田金荣), Ke-Xuan Li(李克轩), Yan-Rong Song(宋晏蓉)
Chin. Phys. B, 2017, 26 (**1**): 014207. DOI: 10.1088/1674-1056/26/1/014207

Modeling of cascaded high isolation bidirectional amplification in long-distance fiber-optic time and frequency synchronization system*

Kuan-Lin Mu(穆宽林)[1], Xing Chen(陈星)[2], Zheng-Kang Wang(王正康)[1], Yao-Jun Qiao(乔耀军)[1,†], and Song Yu(喻松)[2,‡]

[1] *The State Key Laboratory of Information Photonics and Optical Communications, School of Information and Communication Engineering, Beijing University of Posts and Telecommunications, Beijing* 100876, *China*

[2] *School of Electronic Engineering, Beijing University of Posts and Telecommunications, Beijing* 100876, *China*

(Received 18 February 2021; revised manuscript received 15 March 2021; accepted manuscript online 23 March 2021)

We propose a physical model of estimating noise and asymmetry brought by high isolation Bi-directional erbium-doped fiber amplifiers (Bi-EDFAs), no spontaneous lasing even with high gain, in longdistance fiber-optic time and frequency (T/F) synchronization system. It is found that the Rayleigh scattering noise can be suppressed due to the high isolation design, but the amplified spontaneous emission (ASE) noise generated by the high isolation Bi-EDFA and the bidirectional asymmetry of the transmission link caused by the high isolation Bi-EDFA will deteriorate the stability of the system. The calculated results show that under the influence of ASE noise, the frequency instability of a 1200 km system composed of 15 high isolation Bi-EDFAs is $1.773 \times 10^{-13}/1$ s. And the instability caused by asymmetry is $2.6064 \times 10^{-16}/30000$–$35000$ s if the total asymmetric length of the bidirectional link length is 30 m. The intensity noises originating from the laser and detector, the transfer delay fluctuations caused by the variation in ambient temperature and the jitter in laser output wavelength are also studied. The experiment composed of three high isolation Bi-EDFAs is done to confirm the theoretical analysis. In summary, the paper shows that the short-term instability of the T/F synchronization system composed of high isolation Bi-EDFAs is limited by the accumulation of ASE noise of amplifiers and the laser frequency drift, while the long-term instability is limited by the periodic variation in ambient temperature and the asymmetry of the amplifiers. The research results are useful for pointing out the direction to improve the stability of the fiber-optic T/F synchronization system.

Keywords: time and frequency synchronization, erbium-doped fiber amplifier, instability, Allan deviation

PACS: 42.65.Yj, 42.60.Da, 42.79.−e, 07.60.Vg **DOI:** 10.1088/1674-1056/abf105

1. Introduction

The problem of transferring precision time and frequency (T/F) signals to a remote location is important in many areas, involving commercial applications and scientific experiments (e.g., telecommunications, metrology, navigation, and geodesy). Comparing with the satellite link, the optical fiber has recently attracted much attentions to build link for T/F synchronization.[1–3] A number of projects have confirmed that T/F synchronization based on optical fiber link can achieve higher transmission accuracy.[4–7]

In order to realize long-distance T/F synchronization, the power loss caused by transmission should be compensated for significantly improving the signal-to-noise ratio (SNR) of the detected signal. Currently, several papers used the single path bi-directional amplifier (SPBA), which has a simple structure, to amplify bidirectional signals in the same erbium-doped fiber (EDF).[8,9] However, the cascaded bidirectional operation by SPBA typically restricts the maximum gain to around 20 dB to avoid spontaneous lasing due to Rayleigh back-scattering and back-reflections.[10–13] High isolation Bi-directional erbium-doped fiber amplifier (Bi-EDFA),[14,15] which usually includes filters and unidirectional isolators, can also be used to compensate the power attenuation in the system. It uses two pieces of EDFs to amplify the forward and backward signals, respectively. Though the high isolation Bi-EDFAs destroy the symmetry of the two-way link to a certain extent, high gain can be obtained with no spontaneous lasing as the filters and unidirectional isolators are used. So, the high isolation Bi-EDFAs are helpful for the ultra-long distance fiber-optic T/F transmission.

In addition to studying the structures of the amplifiers to realize long-distance T/F synchronization in optical fiber link, it is also necessary to analyze the noises in the system to improve the stabilities of the transmitted time and frequency signals. Usually, the method of experimental measurement or modeling can be used to analyze the fiber-optical T/F system. The experimental measurement can provide accurate performance index of the system, but it usually takes a long time (e.g., several days). And the data obtained by experimental measurement usually only reflect the overall performance of the system which can not show the influence of each indepen-

*Project supported by the National Natural Science Foundation of China (Grant Nos. 61701040, 61771062, and 61871044), the Youth Program of the National Natural Science Foundation of China (Grant No. 61901046), the Fundamental Research Funds for the Central Universities, China (Grant Nos. 2019XD-A18 and 2019PTB-004), and the Youth Research and Innovation Program of BUPT (Grant No. 2017RC13).

†Corresponding author. E-mail: qiao@bupt.edu.cn

‡Corresponding author. E-mail: yusong@bupt.edu.cn

© 2021 Chinese Physical Society and IOP Publishing Ltd

dent devices. Through modeling method, we can understand the influence of each independent devices on the instability of the transmitted time and frequency signals from the physical mechanism, compare the noises introduced by the devices and point out the direction for improving the instability of the system. In 2012, Śliwczyński and Kołodziej[16] have proposed the method of estimating the intensity noises induced by fiber and SPBAs in two-way fiber-optic T/F transfer system, and Li *et al.*[17] used the same method to analyze the noise sources in 200 km optical fiber link. Except for the intensity noises, some other research work has focused on the impact of the transfer delay fluctuations upon the T/F transfer instability. It was found that the transfer delay fluctuations caused by the variation of refractive index, the variation of fiber link length, and the drift of laser output wavelength are major factors of reducing the instability of T/F synchronization.[18,19] The main factors that affect the instability, including the intensity noises and transfer delay fluctuation caused by various variations, are given in the above papers, but no systematic analysis in a long-distance fiber-optic synchronization system which signal attenuation is compensated by the high isolation Bi-EDFAs.

In this paper, we will do the research on the intensity noises and transfer delay fluctuations in fiber-optic T/F synchronization system which signal attenuation is compensated by the high isolation Bi-EDFAs. The structure of long-distance optical fiber chain and our high isolation Bi-EDFAs for T/F synchronization have been shown. The intensity noises which originate from the amplifiers, laser and detector are first analyzed in Section 2. Comparing with the system amplified by SPBAs, the single Rayleigh backscattering noise, double Rayleigh backscattering noise and the backscattered amplified spontaneous emission (ASE) noise can be removed for one-way isolators and wavelength division multiplexers (WDMs) that used in our high isolation Bi-EDFAs. Then the transfer delay fluctuations caused by the variation in ambient temperature and the jitter in laser output wavelength are also studied. The calculated results show that the instability for a 1200 km free-running T/F synchronization system decreases first, from 2.7233×10^{-12} ($\tau\sim1$ s) to 7.9205×10^{-14} ($\tau\sim54$ s), and then increases to 2.0851×10^{-11} with the average interval time enlarged to approximately 30000–35000 s. In Section 3, we will discuss the impact of the amplifiers' asymmetry on the performance of the T/F synchronization system. The instability caused by asymmetry is $\sigma(\tau\sim30000$–$35000\text{ s})=2.6064\times10^{-16}$ if the total asymmetric length of the bidirectional link length is 30 m. A free-running frequency synchronization system, including three high isolation Bi-EDFAs, is carried out to verify the analysis in Section 4. The measured results show that the instability for a 125.58 km free-running frequency synchronization system is $\sigma(\tau\sim1\text{ s})=2.7521\times10^{-13}$, $\sigma(\tau\sim400\text{ s})=1.3674\times10^{-13}$.

2. Modeling of the instability of T/F synchronization system based on the high isolation Bi-EDFAs

When the transmission distance exceeds several dozen of kilometers, it is necessary to regenerate the signal, usually by using the EDFAs. The diagram showing the long-distance chain for T/F transmission with N segments of optical fibers and high isolation Bi-EDFAs is presented in Fig. 1. In the laser transmitters (Tx) at both A and B sides of the link, the T/F signals (e.g., 1 pps, 2.4 GHz) supplied by local atomic clocks are coded on the optical carrier which is generated by a standard fiber laser or semiconductor laser. Then the signal is sent from Tx to the receiver (Rx) through the optical fiber link to discriminate, and the power loss is compensated by the high isolation Bi-EDFAs. In case of the time transfer, the 1-pps signal is next extracted from this discriminated waveform, whereas in case of the frequency transfer, this directly forms the output from the link. Then, both local and remote signals might be compared in a usual way, by using, e.g., the phase comparator or the time interval counter.

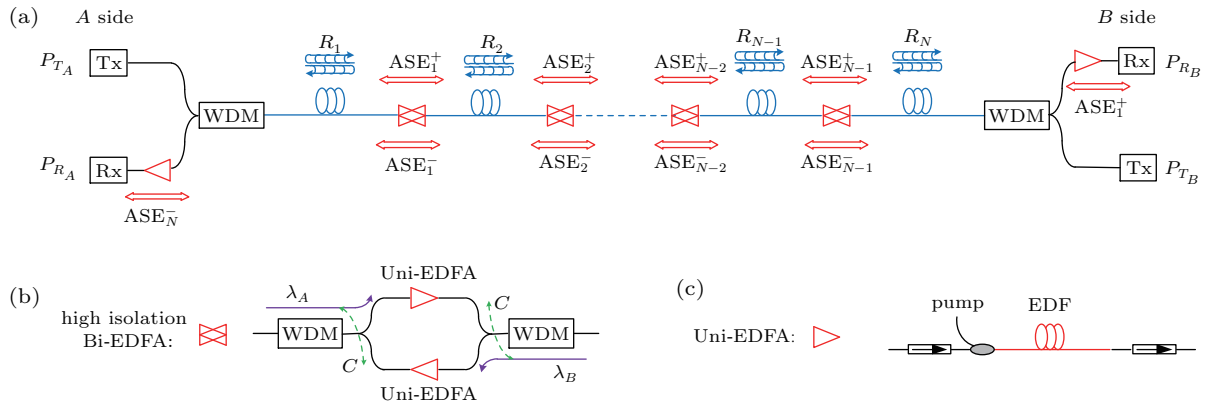


Fig. 1. System structure diagram: (a) Long-distance link of optical fiber spans based on cascaded high isolation Bi-EDFAs for T/F synchronization. (b) Structure diagram of high isolation Bi-EDFA. There is about −45 dB crosstalk between adjacent channels of WDM, as shown by the dotted line in the figure. (c) Structure diagram of Uni-EDFA. WDM: wavelength division multiplexer, EDF: erbium-doped fiber.

2.1. Instability caused by intensity noise of the T/F synchronization system

Causes of stability degradation are the cumulative intensity noise and transfer delay fluctuation in the synchronous networks. Here, we first discuss the intensity noise which originates from the link (including fibers and the high isolation Bi-EDFAs), laser and detector.

2.1.1. Instability caused by intensity noise of the fiber and cascaded high isolation Bi-EDFAs

Considering the schematic diagram presented in Fig. 1, we should study the interfering signals from Rayleigh backscattering (marked as $R_{1,\ldots,N}$) and ASE noise (marked as $\mathrm{ASE}^{+}_{1,\ldots,N}$ and $\mathrm{ASE}^{-}_{1,\ldots,N}$, here $\mathrm{ASE}^{+}_{1,\ldots,N}$ are the ASE noise of the Uni-EDFAs used in $A\rightarrow B$ transmission and $\mathrm{ASE}^{-}_{1,\ldots,N}$ are the ASE noise of the Uni-EDFAs used in $B\rightarrow A$ transmission) which will impinge the receiver together with the desired signal.

Taking the optical signal emitted by A side as an example and focusing only on the most intense components, we may write the power received at the B side of the link as

$$\begin{aligned} P_{R_B} &= P_{B\leftarrow A}+P_{T_B,\mathrm{BSE}}+P_{T_A,\mathrm{BDE}}+P^{+}_{\mathrm{ASE}} \\ &\quad +P^{+}_{\mathrm{ASE-BSE}}+P^{-}_{\mathrm{ASE}}+P^{-}_{\mathrm{ASE-BSE}}, \end{aligned} \tag{1}$$

where $P_{B\leftarrow A}$ is the desired signal transmitted from A side to B side, and the other terms in Eq. (1) designate unwanted interfering signals: $P_{T_B,\mathrm{BSE}}$, single Rayleigh backscattering of the light output from the laser at B side, $P_{T_A,\mathrm{BDE}}$, double Rayleigh backscattering of the light output from the laser at A side, $P^{\pm}_{\mathrm{ASE}}$, ASE noise of the EDFAs, and $P^{\pm}_{\mathrm{ASE-BSE}}$,the backscattered ASE noise. Based on the model shown in Fig. 1, the powers of the items in Eq. (1) can be calculated by using the following formulas:

$$P_{B\leftarrow A} = P_{T_A}\prod_{i=1}^{N} AN_iG_i, \tag{2}$$

$$\begin{aligned} P_{T_B,\mathrm{BSE}} &= P_{T_B}R_NCG^{+}_N+\sum_{i=1}^{N-1}P_{T_B}\left(\prod_{j=i}^{N-1}AN_{j+1}G^{-}_j\right) \\ &\quad \times R_i\left(\prod_{k=i}^{N-1}AN_{k+1}\left(C^2G^{+}_k+D^2G^{-}_k\right)\right)CG^{+}_N, \end{aligned} \tag{3}$$

$$\begin{aligned} P_{T_A,\mathrm{BDE}} &= \sum_{i=1}^{N-1}P_{T_A}\left(\prod_{j=1}^{N-1}AN_jG^{+}_j\right)R_{i+1}\left(C^2G^{-}_i+D^2G^{+}_i\right) \\ &\quad \times R_iG^{+}_i\left(\prod_{k=i}^{N-1}AN_{k+1}G^{+}_{k+1}\right), \end{aligned} \tag{4}$$

$$P^{+}_{\mathrm{ASE}} = \sum_{i=1}^{N-1}\mathrm{ASE}_{+,i}\prod_{j=i}^{N-1}AN_{j+1}G^{+}_{j+1}+\mathrm{ASE}_{+,N}, \tag{5}$$

$$\begin{aligned} P^{+}_{\mathrm{ASE-BSE}} &= \sum_{i=1}^{N-1}\mathrm{ASE}_{+,i}DR_i\prod_{j=i}^{N-1}AN_{j+1}G^{+}_{j+1} \\ &\quad +\mathrm{ASE}_{+,N}DR_NG^{+}_N, \end{aligned} \tag{6}$$

$$\begin{aligned} P^{-}_{\mathrm{ASE}} &= \sum_{i=1}^{N-1}\mathrm{ASE}_{+,i}D\prod_{j=i}^{N-1}AN_{j+1} \\ &\quad \times\left(D^2G^{-}_{j+1}+C^2G^{+}_{j+1}\right), \end{aligned} \tag{7}$$

$$P^{-}_{\mathrm{ASE-BSE}} = \sum_{i=1}^{N-1}\mathrm{ASE}_{+,i}R_i\prod_{j=i}^{N}AN_{j+1}\left(D^2G^{-}_j+C^2G^{+}_j\right). \tag{8}$$

Here, AN is the attenuation of the fiber, G is the gain of the amplifier, and C is the channel crosstalk coefficient of WDM. Our test results show that $C=-45$ dB when the lasers wavelength from A and B sides are in adjacent channels, and there is no crosstalk when non-adjacent channels are used. D is the isolation degree of the isolator, and the isolation degree used in our amplifier is 42 dB. P_{T_A} is the optical power of the laser transmitter at A side. The loss of an individual fiber is estimated by the relation $AN_i=\exp(-\alpha_il_i)$, where l_i is the fiber length and α_i is the attenuation coefficient. The power of ASE can be calculated as $\mathrm{ASE}=2n_{\mathrm{sp}}(G-1)h\nu B_{\mathrm{opt}}$, where n_{sp} is the inversion parameter of erbium particles, h is the Planck's constant, ν is the frequency of light and B_{opt} is the optical bandwidth. In order to obtain the specific magnitude of the items in Eq. (1), we set $P_{T_A}=P_{T_B}=1$ mW, $\alpha=0.2$ dB/km, $n_{\mathrm{sp}}=0.6$, and $B_{\mathrm{opt}}=100$ GHz. The calculated results are shown in Table 1.

Table 1. Calculated power values of the optical signals.

Adjacent channels of WDM are used: $C=-45$ dB

Terms	$P_{B\leftarrow A}$	$P_{T_B,\mathrm{BSE}}$	$P_{T_A,\mathrm{BDE}}$	P^{+}_{ASE}	$P^{+}_{\mathrm{ASE-BSE}}$	P^{-}_{ASE}	$P^{-}_{\mathrm{ASE-BSE}}$
Power (mW)	1	1.05×10^{-6}	1.09×10^{-10}	1.58×10^{-2}	3.31×10^{-8}	4.5×10^{-8}	2.49×10^{-15}

Non-adjacent channels of WDM are used: $C=0$

Terms	$P_{B\leftarrow A}$	$P_{T_B,\mathrm{BSE}}$	$P_{T_A,\mathrm{BDE}}$	P^{+}_{ASE}	$P^{+}_{\mathrm{ASE-BSE}}$	P^{-}_{ASE}	$P^{-}_{\mathrm{ASE-BSE}}$
Power (mW)	1	0	8.72×10^{-11}	1.58×10^{-2}	3.31×10^{-8}	5×10^{-8}	1.99×10^{-15}

We can see that compared with $P_{B\leftarrow A}$ and P^{+}_{ASE}, the values of $P_{T_B,\mathrm{BSE}}$, $P_{T_A,\mathrm{BDE}}$, $P^{+}_{\mathrm{ASE-BSE}}$, P^{-}_{ASE}, and $P^{-}_{\mathrm{ASE-BSE}}$ can be ignored. This is why the spontaneous lasing can be suppressed even the high isolation Bi-EDFAs work in high gain state.

The optical signal which is given by Eq. (1) impinges the photodiode and generates electrical current, including some noise components apart from the useful signal. The current generated by the photodiode is proportional to the square of

the amplitude of the electric field. Hence, we may write the equation for the electric signal in the B side receiver as

$$I_{R_B} \sim |E_{B\leftarrow A}|^2 + |E_{\rm ASE}|^2 + 2{\rm Re}\{E_{B\leftarrow A}\cdot E_{\rm ASE}\}. \quad (9)$$

Equation (9) includes three terms where only the first one is responsible for transferring the T/F signal and other two terms should be regarded as noises, which will degrade the SNR of received signal. The second term results from the self-beating of the ASE noise, which with the variance is dependent on the electrical bandwidth $B_{\rm el}$ and the optical bandwidth $B_{\rm opt}$. The last term is simply the signal-ASE beating noise. The expressions of the electrical noises are summarized in Table 2. $\Re$ is the responsivity of the photodiode.

Table 2. Electrical noises resulting from Eq. (9).

Term No.		ε_i^2	Description
2	$\lvert E_{\rm ASE}\rvert^2$	$(\Re P_{\rm ASE})^2 \frac{(2B_{\rm opt}-B_{\rm el})B_{\rm el}}{2B_{\rm opt}^2}$	$P_{\rm ASE}$ self-beating
3	$2{\rm Re}\{E_{B\leftarrow A}\cdot E_{\rm ASE}\}$	$4\Re^2 P_{B\leftarrow A}P_{\rm ASE}\frac{B_{\rm el}}{B_{\rm opt}}$	$P_{B\leftarrow A}-P_{\rm ASE}$ beating

Having recognized the useful signal and the main noise sources, the SNR of received signal at the Rx side can be estimated as

$${\rm SNR}_{\rm I,1} = \frac{(\Re\cdot P_{B\leftarrow A})^2}{\kappa_2\varepsilon_2^2+\kappa_3\varepsilon_3^2}, \quad (10)$$

where κ_2 and κ_3 in the denominator denote the relative polarization between the electric fields beating in the detector. Then the Allan deviation denoting the instability can be obtained as[20,21]

$$\sigma_{\rm I,1}(\tau) = \frac{\sqrt{3}}{2\pi\nu_0\tau m\sqrt{{\rm SNR}_{\rm I,1}}}. \quad (11)$$

Some illustrative examples are presented here to obtain an insight into the general performance of the discussed T/F synchronization system. For calculations, $B_{\rm el}=15$ MHz, $\nu_0=2.4$ GHz, $m=1$, $\Re=1$, and $\kappa_2=\kappa_3=0.5$.

More number of the high isolation Bi-EDFAs must be used to compensate the attenuation of longer link, and the distances between the amplifiers may vary. In order to simplify the analysis process, we simulate the SNR and instability degraded by the intensity noise of the fiber, the amplifiers in the assumption of the distances between the high isolation Bi-EDFAs are equal, and the gain of each amplifier just compensates the attenuation of the previous optical link. The curves in Fig. 2(a) show the trend of $\rm SNR_{I,1}$ with the increase of link length in three cases of distance between amplifiers (i.e., 40 km, 60 km, and 80 km). The curves in Fig. 2(b) are the Allan deviation denoting the instability with an average interval time of 1 s. The curves in Fig. 2(c) denote the Allan deviation as a function of average interval time, when the total length of the link is fixed to 1200 km, where the number of amplifiers are 30, 20, and 15 for the fiber length of per segment as 40 km, 60 km, and 80 km, respectively.

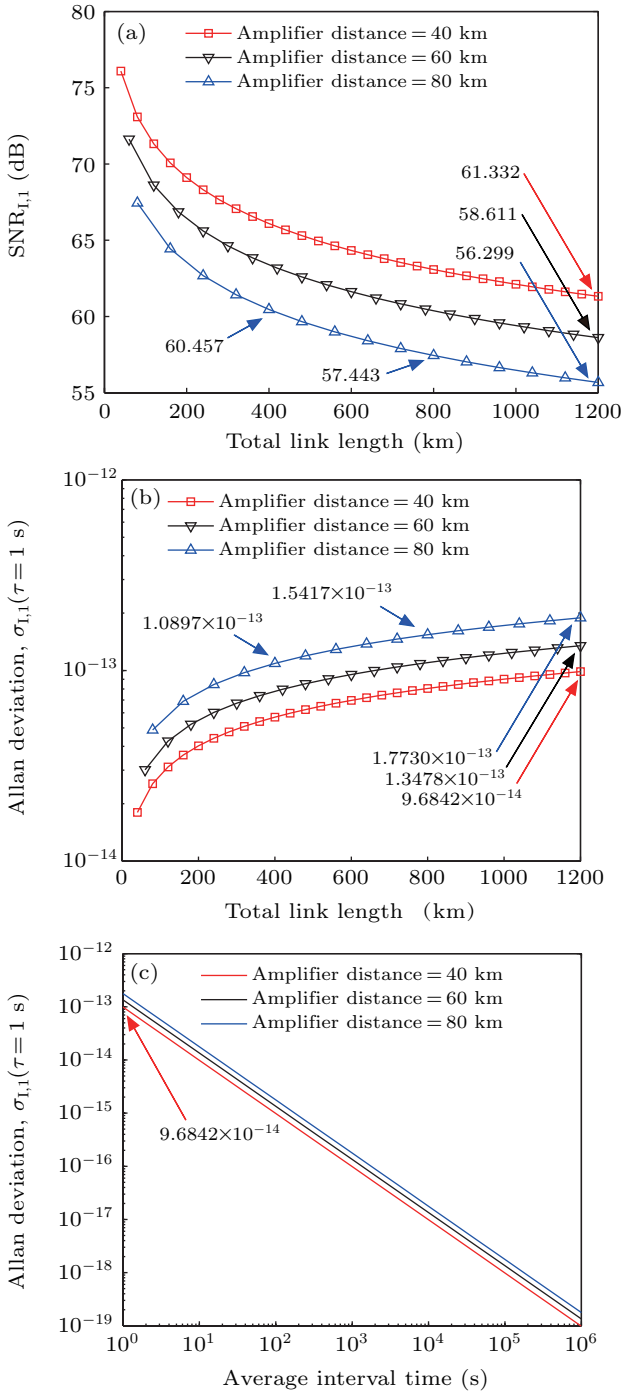


Fig. 2. Performance of T/F synchronization system versus the intensity noise of the fiber and cascaded high isolation Bi-EDFAs: (a) SNR of the received signal versus the total link length; (b) Allan deviation of instability with an average interval time of 1 s versus the total link length; (c) Allan deviation as a function of average interval time for fixed 1200 km link length.

As can be seen from Fig. 2, with the increase of the link length, the number of amplifiers required will increase correspondingly, resulting in the accumulation of ASE noise. Therefore, the longer the link length is, the smaller the SNR of the received signal, which leads to a worse performance of the T/F synchronization system. For example, in the case

of 400 km and 800 km link length where the distance of per segment is 80 km, the simulation results of SNRs are 60.457 dB and 57.443 dB, and the calculated Allan deviations are 1.0897×10^{-13} and 1.5417×10^{-13} ($\tau=1$ s), respectively. Another feature is that the distance between the high isolation Bi-EDFAs in the link should not be too long-for the ASE noise is directly proportional to the gain of the amplifier. For the same link length of 1200 km, the SNRs of the received signals are 61.322 dB, 58.611 dB and 56.229 dB for amplifiers distance of 40 km, 60 km and 80 km, and the corresponding Allan deviations are 9.6842×10^{-14}, 1.3478×10^{-13} and 1.773×10^{-13} ($\tau=1$ s), respectively. So when the power attenuation of the useful signal from A side is just compensated, the SNR of the received signal (including the useful signal and the intensity noise) can be optimized by reducing the distances of the amplifiers. The trend of Allan deviation is linear and inversely proportional to the average interval time as can be seen from Fig. 2(c).

2.1.2. Instability caused by other intensity noise of laser and detector

The conversion of the laser phase noise into the intensity modulation (PM-IM) noise occurs because of the chromatic dispersion of the fiber, and the relative intensity noise (RIN) of the laser should be considered. They can be expressed as[16,21]

$$\varepsilon^2_{\mathrm{PM-IM}} = \frac{(\Re P_{B\leftarrow A})^2}{\pi}\int_0^\infty |H(f)|^2\frac{2\Delta v}{\Delta v^2+f^2}\left(1-\exp(-\psi\cdot\Delta v)\times\left(\cos(\psi\cdot v)+\frac{\Delta v}{f}\sin(\psi\cdot v)\right)\right)\mathrm{d}f, \tag{12}$$

$$\varepsilon^2_{\mathrm{RIN}} = e^2\left(\frac{\Re P}{hv}\right)^2 n_{\mathrm{RIN}}B_{\mathrm{el}}, \tag{13}$$

where $\psi=2\pi\lambda D_{\mathrm{T}}$, $\lambda=1550$ nm is the wavelength of the laser, $\Delta v=30$ KHz is the spectral linewidth of the laser, and $D_{\mathrm{T}}=\left|\sum_{i=0}^{N}D_i\cdot l_i\right|$ is accumulated chromatic dispersion of the link, while $D_i=17$ ps/(nm·km) is the dispersion coefficient, and l_i denotes the fiber length. The transfer characteristic of the receiver is denoted as $H(f)$.

And for the detector, thermal noise ($\varepsilon^2_{\mathrm{th}}=4kTB_{\mathrm{el}}/R_{\mathrm{L}}$) and shot noise ($\varepsilon^2_{\mathrm{shot}}=2\mathrm{e}^2(\Re P/hv)B_{\mathrm{el}}$) are two main noises that can not be ignored in the analysis process.[21] Here, $k=1.3806515\times10^{-23}$ J/K is Boltzman's constant, $T=296$ K denotes the temperature and $R_{\mathrm{L}}=50\ \Omega$ represents the load resistance of the detector.

Having recognize the main intensity noise of laser and receiver, we may define the $\mathrm{SNR}_{\mathrm{I,2}}$ and $\sigma_{\mathrm{I,2}}(\tau)$ as below:

$$\mathrm{SNR}_{\mathrm{I,2}} = \frac{(\Re\cdot P_{B\leftarrow A})^2}{\varepsilon^2_{\mathrm{PM-IM}}+\varepsilon^2_{\mathrm{RIN}}+\varepsilon^2_{\mathrm{th}}+\varepsilon^2_{\mathrm{shot}}}, \tag{14}$$

$$\sigma_{\mathrm{I,2}}(\tau) = \frac{\sqrt{3}}{2\pi v_0\tau m\sqrt{\mathrm{SNR}_{\mathrm{I,2}}}}. \tag{15}$$

Figure 3 shows the calculated instability results caused by intensity noises of laser and detector. We can see the instability result is about 1.1189×10^{-14} with average interval time of 1 s, which is smaller than that of 9.6842×10^{-14} denoted by the red line in Fig. 2(c). The comparison results shows that the ASE noise introduced by the amplifier has more serious influence on the stability of the signals transmitted by the T/F synchronization system than that of the intensity noises introduced by laser and detector.

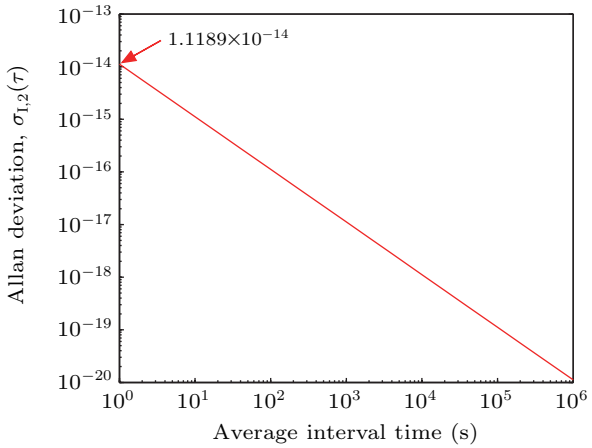


Fig. 3. Performance of T/F synchronization system versus the intensity noises of laser and detector. The link length is set as $30\times40=1200$ km, 30 is the number of amplifiers and 40 km is the fiber length between amplifiers.

2.2. Instability caused by transfer delay fluctuation

Starting from the equation for the fiber propagation delay $\tau=Ln/c$, where L is the link length, n is the group refractive index and c is the velocity of light in vacuum.[18] As we know, the fiber length and refractive index will change with the temperature variation, resulting in the fluctuation of transfer delay time. Sinusoidal curve can be used to model the change of ambient temperature with time as $\Delta T(t)=A\sin(2\pi t/T_1)$,[20] where A denotes the amplitude, and T_1 (usually can be set as 1 day) is the period. Thus the Allan variance denoting the instability caused by temperature change in the length of optical fiber link can be calculated as follows:[21,22]

$$\sigma^2_{\mathrm{D,1}}(\tau)=\left(\frac{nLA}{c}\frac{\partial\Delta L}{\partial T}\right)^2\frac{4}{\tau^2}\left(\sin\left(\frac{\pi\tau}{T_1}\right)\right)^4. \tag{16}$$

Similarly, the Allan variance denoting the instability induced by the temperature change in the refractive index can also be expressed as[21,22]

$$\sigma^2_{\mathrm{D,2}}(\tau)=\left(\frac{nLA}{c}\frac{\partial\Delta n}{\partial T}\right)^2\frac{4}{\tau^2}\left(\sin\left(\frac{\pi\tau}{T_1}\right)\right)^4, \tag{17}$$

where $\partial\Delta L/\partial T$ and $\partial\Delta n/\partial T$ are the variation coefficients of fiber length and refractive index following with temperature, respectively.

In Fig. 4, the graphs of instability versus the transfer delay fluctuation caused by the link are drawn with the lines. The curves in Figs. 4(a) and 4(b) show instabilities which are affected by delay fluctuation introduced by the fiber length and fiber refractive index variation with temperature. Here, the link length is set to 400, 800, and 1200 km, respectively. The temperature change amplitude is selected to be 10 or 0.1 degrees Celsius for the impact of the environmental temperature change on the fiber link will be reduced by 99% after the fiber is buried underground. The fiber group refractive index is set as $n = 1.45$.

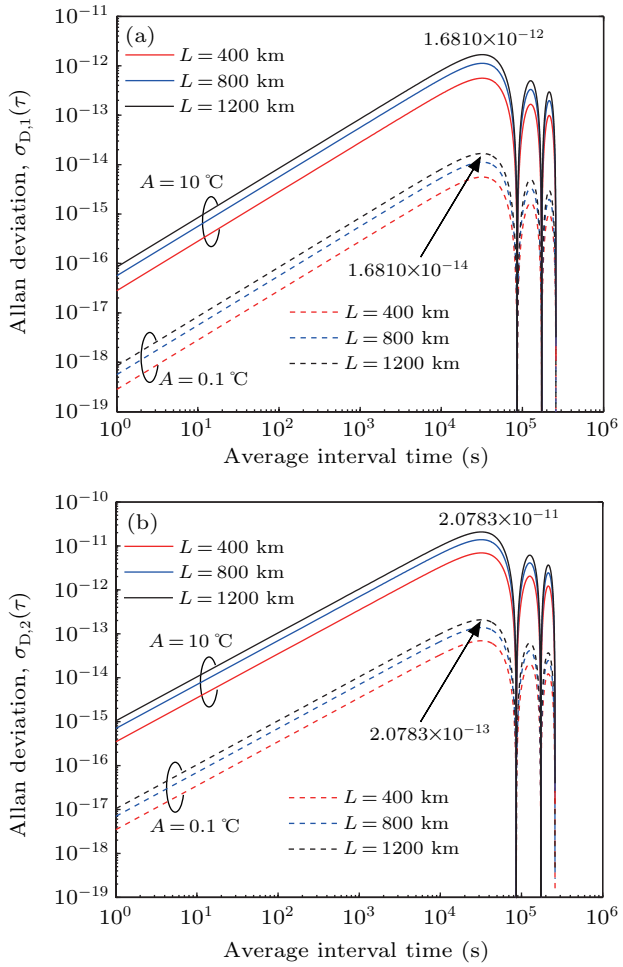


Fig. 4. Instability which is impacted by temperature fluctuation. (a) Instability which is impact by transfer delay fluctuation introduced by the fiber length variation following with temperature. (b) Instability which is impact by transfer delay fluctuation introduced by the fiber refractive index variation following with temperature.

As can be seen from Figs. 4(a) and 4(b), in the short term, the Allan deviation $\sigma_{D,1}(\tau)$ and $\sigma_{D,2}(\tau)$ are proportionally degraded to average interval time τ and link length L, and they reach the maximum where τ is enlarged to approximately 30000–35000 s. The value of $\sigma_{D,1}(\tau)$ is less than that of $\sigma_{D,2}(\tau)$ for $\partial(\Delta L)/\partial T = 5.5\times10^{-7}$ °C^{-1} is smaller than $\partial(\Delta n)/\partial T = 6.8\times10^{-6}$ °C^{-1}. For a link length of $L =$ 1200 km and temperature fluctuation range of $A = 10$ °C, the peak value of $\sigma_{D,1}(\tau)$ and $\sigma_{D,2}(\tau)$ are about 1.6810×10^{-12} and 2.0783×10^{-11}, respectively. If the temperature fluctuation range decreases to $A = 0.1$ °C, the peak value of $\sigma_{D,1}(\tau)$ and $\sigma_{D,2}(\tau)$ will upgrade to about 1.6810×10^{-14} and 2.0783×10^{-13} at the same average interval time of approximately 30000–35000 s, respectively. When τ is larger than 3.5×10^{4} s, the Allan deviation decreases, and it becomes zero at one day, as well as its multiple numbers, because the temperature fluctuation is canceled under the assumption of sinusoidal curve.

The propagation time also depends on the wavelength of transmission signal via wavelength dependency of refractive index. So the laser frequency drift will also cause the jitter of the transmission signal delay in the T/F synchronization system. Chen *et al.*[21,23] have given out the Allan variance expression of instability caused by distributed feedback (DFB) laser wavelength drift in the fiber refractive index by integrating the frequency fluctuation noise PSD of a semiconductor laser, using $S_v(v) = (K/v) + (\Delta v/\pi)$,[24] as follow:

$$\sigma^2_{D,3}(\tau) = \left(\frac{2\pi L\lambda^2}{c}\frac{dn}{d\lambda}\right)^2 \times\left(\frac{K(1.038+3\ln(2\pi v_H\tau))}{4\pi^2\tau^2}+\frac{\Delta v}{\pi}\frac{3v_H}{4\pi^2\tau^2}\right). \quad (18)$$

The total Allan variance for instability caused by transfer delay fluctuations can be obtained as[25]

$$\sigma^2_D(\tau) = \sigma^2_{D,1}(\tau)+\sigma^2_{D,2}(\tau)+\sigma^2_{D,3}(\tau). \quad (19)$$

Calculated instability results caused by transfer delay fluctuations using Eq. (19) are shown in Fig 5. Here, the link length is set as 1200 km. The temperature fluctuation range is set as $A = 10$ °C.

As can be seen from the simulation results in the Fig. 5, in the free-running situation, the output wavelength jitter of the laser mainly affects the short-term instability of the system, while the periodic change of temperature mainly degrades the long-term instability of the system.

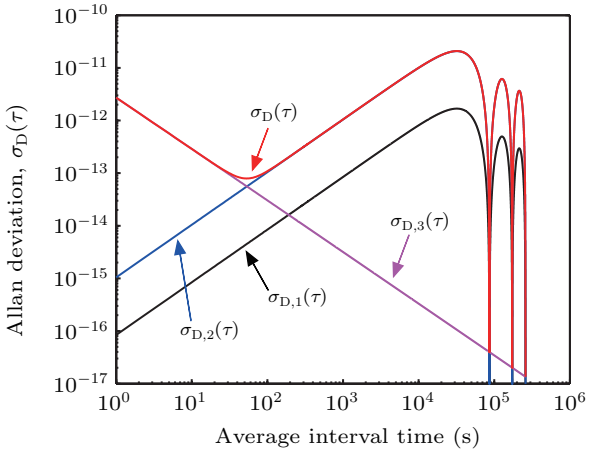


Fig. 5. Calculated instability results caused by transfer delay fluctuations.

2.3. The total Allan deviation of the system

Finally, the performance of the free-running T/F synchronization system can be valued by summarizing the calculated results of $\sigma_{\mathrm{I}}(\tau)$ and $\sigma_{\mathrm{D}}(\tau)$, corresponding to the factors of intensity noise and transfer delay fluctuations as below:

$$\begin{aligned}\sigma^2_{\mathrm{Total}}(\tau) &= \sigma^2_{\mathrm{I}}(\tau)+\sigma^2_{\mathrm{D}}(\tau)\\ &= \sigma^2_{\mathrm{I},1}(\tau)+\sigma^2_{\mathrm{I},2}(\tau)\\ &\quad+\sigma^2_{\mathrm{D},1}(\tau)+\sigma^2_{\mathrm{D},2}(\tau)+\sigma^2_{\mathrm{D},3}(\tau).\end{aligned} \tag{20}$$

In Fig. 6(a), the black line is the instability result caused by intensity noise which originates from the laser, fiber, amplifier and detector. The blue line is the instability caused by transfer delay fluctuations. Though the red curve almost coincides with the blue curve, the red curve denotes the total Allan deviation of the free-running system. The total Allan deviation denotes the instability decreases first, from 2.7233×10^{-12} ($\tau=1$ s) to 7.9205×10^{-14} ($\tau\sim54$ s), and then increases to 2.0851×10^{-11} with the average interval time enlarged to approximately 30000–35000 s. And with the decrease of temperature fluctuation, the inflection point will move to the direction with longer average interval time, and the corresponding stability performance will be improved as shown in Fig. 6(b)

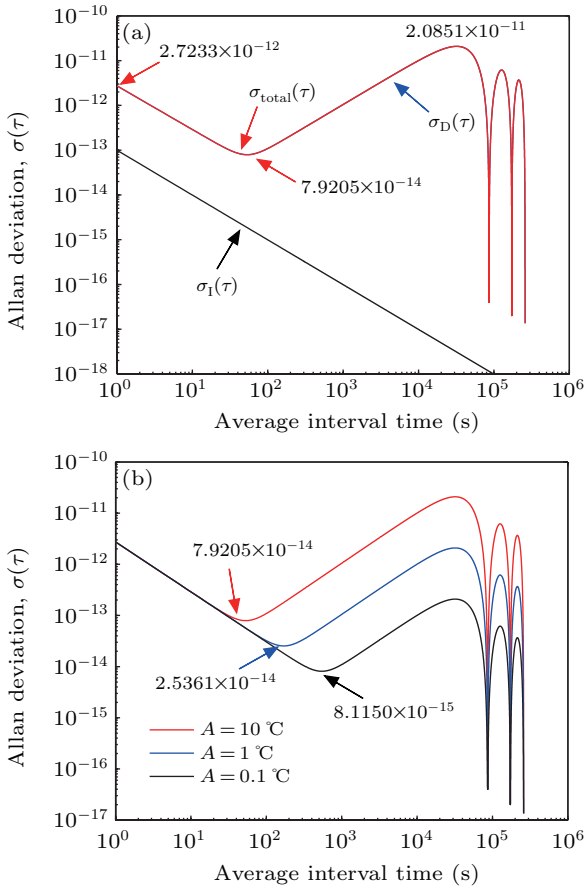


Fig. 6. Total influence of various noises on T/F synchronization performance along $30\times40=1200$ km fiber link, 30 is the number of amplifiers and 40 km is the fiber length between amplifiers: (a) Allan deviation denotes the instability of the free-running T/F synchronization system (the temperature fluctuation range is set as $A=10$ °C); (b) the total instability as a function of different amplitude of temperature fluctuation.

(i.e., 7.9205×10^{-14} ($\tau\sim54$ s) for $A=10$ °C, 2.5361×10^{-14} ($\tau\sim170$ s) for $A=1$ °C and 8.1150×10^{-15} ($\tau\sim545$ s) for $A=0.1$ °C).

As can be seen from the simulation results, the short-term instability of the T/F synchronization system is limited by the accumulated ASE noises of the amplifiers and the frequency stability of the laser. The long-term instability is limited by the temperature fluctuation.

3. Asymmetry caused by the cascaded Bi-EDFAs

In the bidirectional T/F synchronization system, the bidirectional symmetry of the link is desired when we try to compensate the transmission delay fluctuation.[26] The high isolation Bi-EDFA in Fig. 1 uses EDFs, WDMs, pumps and isolators to form two Uni-EDFAs to realize the power compensation. This scheme can avoid spontaneous lasing and provide enough high gain for forward and backward signals in T/F system. However, it is difficult to ensure the consistency of the fiber length of the two Uni-EDFAs in the process of splicing. When multiple amplifiers are used as the relay system, the bidirectional symmetry of the whole link is destroyed. The uncertainty of transfer delay calibration caused by the link asymmetry can be calculated as

$$\sigma_{\mathrm{D}}(\Delta L',\tau)=\frac{1}{2}\left|\sigma^{+}_{\mathrm{D}}(L,\tau)-\sigma^{-}_{\mathrm{D}}(L-\Delta L',\tau)\right|, \tag{21}$$

where $\Delta L'$ denotes total asymmetric length of bidirectional link, $\sigma^{+}_{\mathrm{D}}(L,\tau)$ and $\sigma^{-}_{\mathrm{D}}(L-\Delta L',\tau)$ denote the instability caused by propagation delay fluctuation in forward and backward directions, respectively.

In Fig. 7, the graphs of instability which is impacted by asymmetry caused by Bi-EDFAs are simulated based on Eq. (21). Here the total link length is set as $L=1200$ km, the amplitude of the temperature fluctuation A is set as 10 °C, and the fiber group refractive index is set as $n=1.45$. Just as shown in Fig. 7, when the total asymmetric length is set

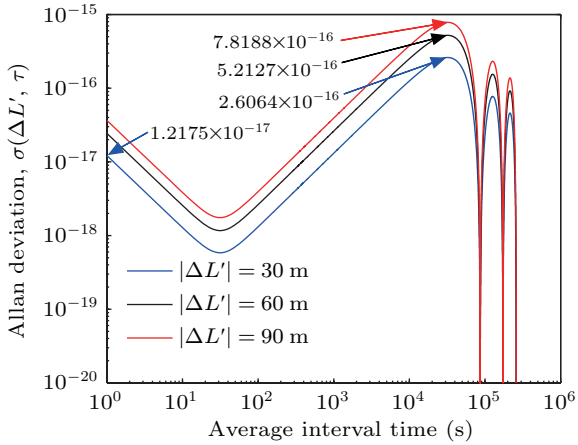


Fig. 7. Instability which is impacted by the asymmetry of the link caused by high isolation Bi-EDFAs.

as $|\Delta L'| = 30$ m, the calculated Allan deviations caused by asymmetry are 1.2175×10^{-17} ($\tau \sim 1$ s) and 2.6064×10^{-16} ($\tau \sim 30000$–35000 s). In addition, the longer asymmetry length will induce more serious impact on the instability of the system. The calculated instabilities are 2.6064×10^{-16}, 5.2127×10^{-16} and 7.8188×10^{-16} ($\tau \sim 30000$–35000 s) when the total asymmetry length are 30, 60 and 90 m, respectively.

Comparing the results shown in Figs. 2(c) and 7, it can be seen that the asymmetry of the Bi-EDFAs has a negligible impact on the short-term performance of the T/F synchronization system. But for large average interval time, around a day or so, the impact of asymmetry of the total link length is comparable with the result that be caused by the SNR of the intensity noise.

4. Experiments

A free-running frequency synchronization system is carried out to verify the analysis and methods presented in the preceding sections. The general measurement setup used during the tests is shown in Fig. 8. A 2.4 GHz RF signal is generated by Agilent E8267D and divided into two signals by electrical coupler for transmission and reference respectively. A laser diode (LD) is modulated with the transmission RF signal through a Mach–Zehnder modulator (MZM). Firstly, three sections of fiber with length of 41.86 km are used and three Bi-EDFAs, shown as Fig. 8(b), are used to compensate the attenuation. Then, three variable optical attenuators (VOAs), shown as Fig. 8(c), are used instead of optical fiber to simulate different link attenuation. In addition, the transmission delay fluctuation caused by the influence of various aspects on the optical fiber are eliminated when VOAs are used. After a manual phase shifter MPS-DC4.2G-180-S, the demodulated 2.4 GHz RF signal received by the PD is mixed with the reference 2.4 GHz signal to detect the phase error. The phase error is transmitted to the voltage value by Keysight 34465A to calculate the Allan deviation.

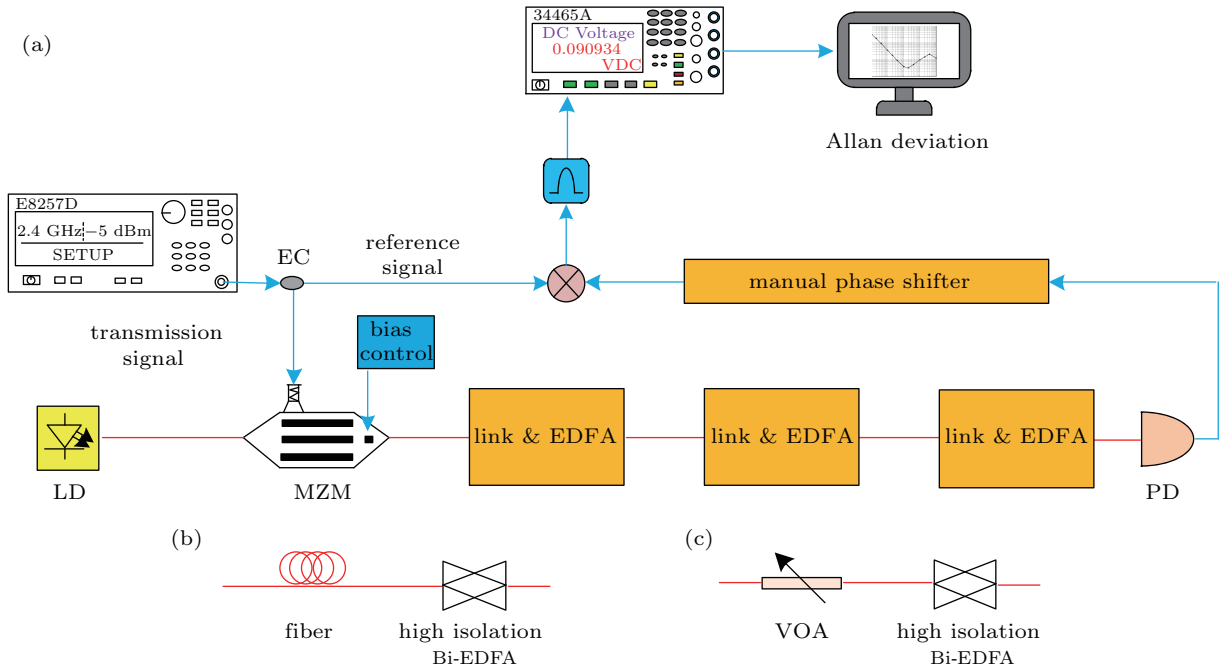


Fig. 8. Experiment diagram of the free-running frequency synchronization system. LD: laser diode, MZM: Mach–Zehnder modulator, VOA: variable optical attenuator, PD: photodiode, EC: electrical coupler.

The experimental Allan deviations denoting the frequency instabilities of the free-running system are shown in Fig. 9. Here, the measured results are $\sigma(\tau = 1\text{ s}) = 1.4548 \times 10^{-14}$, $\sigma(\tau{=}1\text{ s}) = 2.3841 \times 10^{-14}$ and $\sigma(\tau{=}1\text{ s}) = 3.2079 \times 10^{-14}$ when the attenuation values of the VOAs are set as 8 dB, 15 dB and 20 dB, respectively. When three sections 41.86 km optical fibers are used, the instability of the transferred frequency degrades to $\sigma(\tau{=}1\text{ s}) = 2.7521 \times 10^{-13}$. As the experiment is completed in an air-conditioned room, where the amplitude of temperature fluctuations is approximately a few degrees, and the period would be shorter than one day. The red line increases again when the average interval time is just larger than about 20 s and reaches 1.3674×10^{-13} at approximately 400 s.

The experimental data is consistent with the simulation result. The higher gain provided by EDFA, the more noise will be brought to the system, which will deteriorate the stability of the transmitted frequency signal as shown by the pink, blue and black lines. Comparing the pink and red lines in Fig. 9, the instability will just be affected by the intensity noise originat-

ing from the amplifier, laser and detector when VOAs are used, and the transfer delay fluctuation caused by $\sigma_{\mathrm{D}}(\tau)$ should be considered in the real system which is composed of optical fiber.

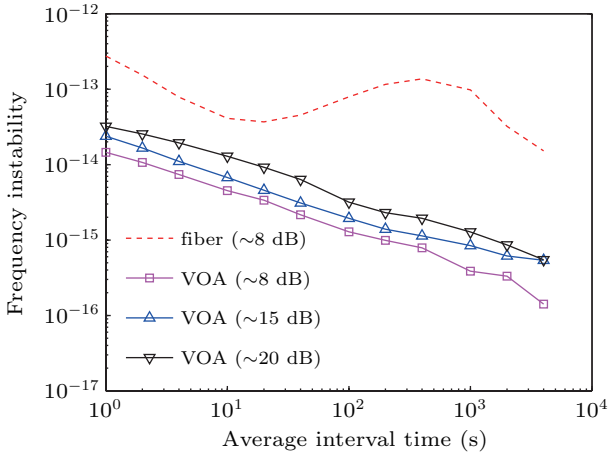


Fig. 9. Instability of the free-running frequency transfer system. The numbers in the parentheses represent the power attenuation bring by fiber link and attenuators.

5. Conclusion

In this paper, we have analyzed the intensity noises and transfer delay fluctuations in the long-distance fiber-optic T/F synchronization system which is based on high isolation Bi-EDFAs. The high isolation Bi-EDFAs use two EDFs, incorporating with direction-separating components in the signal path (e.g., optical isolators and WDMs), to amplify the signals in forward and backward directions, respectively. Compared with the SPBAs, such amplifiers can improve the SNR of the received signal at the remote side by blocking the propagation of backscattered signals which will interfere with transferred T/F signals. And the high isolation Bi-EDFAs can be used to realize the ultra-long distance fiber-optic T/F transmission.

The models presented in this paper takes into account of the intensity noises to estimate the SNR at the receiver of the T/F system, including the ASE noise of the high isolation Bi-EDFAs, the RIN of the laser and the conversion of the laser phase noise into the intensity noise that occurs because of the fiber chromatic dispersion, the thermal noise and shot noise of the detector. We have also considered the transfer delay fluctuations caused by the variation in fiber link length, the variation in refractive index and the jitter in laser output wavelength. The results of the performed research show that the short-term instability of the T/F synchronization system is mainly limited by the ASEs noise and the laser frequency drift, while the long-term instability is limited by the periodic variation of ambient temperature impact on the fiber.

A free-running frequency synchronization experiment has been done with three variable optical attenuators (VOAs), incorporating three high isolation Bi-EDFAs, to prove our theoretical predictions. The measured instability was $\sigma(\tau \sim 1\,\mathrm{s}) = 1.4548 \times 10^{-14}$ when the attenuation values of the three VOAs are set as 8 dB. When three sections of 41.86 km optical fibers are used to instead of the VOAs, the instability of the transferred frequency degraded to $\sigma(\tau \sim 1\,\mathrm{s}) = 2.7521 \times 10^{-13}$ and $\sigma(\tau \sim 400\,\mathrm{s}) = 1.3674 \times 10^{-13}$ for the optical fibers will introduce the transfer delay fluctuations.

The asymmetry caused by the high isolation Bi-EDFAs will deteriorate the long-term instability of the T/F system for the bidirectional transmission delay fluctuations are unequal and can't be fully compensated.

References

[1] Amemiya M, Imae M, Fujii Y, Suzuyama, T, Hong F L and Takamoto M 2010 *IEEE Trans. Instrum. Meas.* **59** 631

[2] Terra O, Groche G and Schnatz H 2010 *Opt. Express* **18** 16102

[3] Lopez O, Kanj A, Pottie P E, Rovera D, Achkar J, Chardonnet C, Amy-Klein A and Santarelli G 2012 *Appl. Phys. B* **110** 3

[4] Kim J, Schnatz H, Wu D S, Marra G, Richardson D J and Slavík R 2015 *Opt. Lett.* **40** 4198

[5] Chen X, Lu J L, Cui Y F, Zhang J, Lu X, Tian X S, Ci C, Liu B, Wu H, Tang T S, Shi K B and Zhang Z G 2015 *Sci. Rep.* **5** 18343

[6] Shang J M, Jiang T W, Liu C X, Chen X, Lu Y M, Yu S and Guo H 2018 *Opt. Express* **26** 33888

[7] Liu C X, Jiang T W, Chen M S, Yu S, Wu R H, Shang J M, Duan J T and Gu W Y 2016 *Opt. Express* **24** 23376

[8] Śliwczyński Ł, Krehlik P, Czubla A, Buczek Łand Lipiński M 2013 *Metrologia* **50** 133

[9] Zhang H, Wu G L, Hu L, Li X M and Chen J P 2015 *IEEE Photon. J.* **7** 1

[10] Raupach S M F, Koczwara A and Grosche G 2014 *Opt. Express* **22** 26537

[11] Calonico D, Bertaccho E K, Calosso C E, Clivati C, Costanzo G A, Frittelli M, Godone A, Mura A, Poli N, Sutyrin D V, Tino G, Zucco M E and Levi F 2014 *Appl. Phys. B* **117** 979

[12] Zhang C, Chen B Q and Li Z Y 2016 *Chin. Phys. B* **25** 095203

[13] Chen L, Yang F R, Su T, Bao W Y, Yan B, Chen S and Li R B 2017 *Chin. Phys. B* **26** 025205

[14] Chen X, Zhang J, Lu J L, Lu X, Tian X S, Liu B, Wu H, Tang T S, Shi K B and Zhang Z G 2015 *Opt. Lett.* **40** 371

[15] Śliwczyński Ł, Krehlik P, Buczek Łand Lipiński M 2012 *IEEE Trans. Instrum. Meas.* **61** 2573

[16] Śliwczyński Łand Kołodziej J 2013 *IEEE Trans. Instrum. Meas.* **62** 253

[17] Li X Y, Zhu Y, Lu L, Li D L and Zeng Z L 2014 *Journal of Military Communications Technology* **35** 17

[18] Śliwczyński Ł, Krehlik P and Lipiński M 2010 *Meas. Sci. Technol.* **21** 075302

[19] Li D L, Cheng Q M, Zhang B F, Lu L, Lei P J and Li X Y 2014 *Laser & Optoelectronics Progress* **51** 010602 (in Chinese)

[20] Primas L E, Logan R T and Lutes G F 1989 *IEEE 43rd Annual Symposium on Frequency Control* Denver, CO, USA, May 31–June 2, 1989, p. 202

[21] Yang F 2013 *Studies on Single-frequency Fiber Laser and Fiber-optic Joint Time and Frequency Transfer* (Ph.D. Dissertation) (Shanghai: Shanghai Institute of Optics and Fine Mechanics Chinese Academy of Sciences) (in Chinese)

[22] Amemiya M, Imae M, Fujii Y, Suzuyama T and Ohshima S 2008 *IEEE Trans. Instrum. Meas.* **57** 878

[23] Chen W, Cheng N, Liu Q, Wang J L, Feng Z T, Fei Y, Han S L, Gui Y Z and Cai H W 2016 *Chinese J. Lasers* **43** 0706001

[24] Kikuchi K 1989 *IEEE J. Quantum Elect.* **25** 684

[25] Liu Q, Chen W, Xu D, Cheng N, Yang F, Gui Y Z, Cai H W and Han S S 2016 *Chinese J. Lasers* **43** 0305006

[26] Liang J X, Liu C X, Hu F, Zhou S J, Yu S and Qiao Y J 2019 *Opt. Commun.* **445** 161